Bounded Model Switching in Uncertain Hybrid Systems

Paul G. Otanez and Mark E. Campbell
Department of Mechanical and Aerospace Engineering
Cornell University
Ithaca, NY 14853
{potanez, mc288}@cornell.edu

Abstract— **The problem of establishing hard bounds on a state estimate of a nonlinear system is described. Within an operating range, the Extended Set-Membership Filter and a set of switched linear models are used in order to minimize the uncertainty on the state estimate. The bounding of the linearization error for use in set-membership with model switching is explained. Methods to select, place, and switch linear models to meet a desired uncertainty are discussed. The proposed methods are then applied to a model of the relative motion of two aircraft.**

I. Introduction

The study of hybrid systems is attractive because many applications can be described in hybrid terms. Although the term *hybrid system* is used for a wide range of systems, it can loosely be defined as a system in which there is interaction of discrete and continuous dynamics. Hybrid systems arise in various engineering applications such as automotive powertrain systems, intelligent vehicle systems, and air traffic management [2], [7], [17]. There has also been interest in hybrid systems among mathematicians and theoretical computer scientists [1]. A more specific definition of a hybrid system is a system described by a set of ordinary differential equations with discontinuities or multivalued right-hand sides [11]. These systems can be used to represent nonlinearities such as saturation, hysteresis, switches, relays, and dead zones. Control laws such as rule-based control, programmable logic control, and gain scheduling are also piecewise linear by nature and fit naturally into the hybrid framework.

State-estimation for hybrid systems has been considered in [15] for piecewise-affine systems, in [6] based on moving-horizon estimation, and in [16] when mode changes are determined by a Markov process. One of the more challenging problems in hybrid estimation is that of sensor scheduling. The problem of minimizing communication by scheduling measurements in stochastic systems is dealt with in [10]. However, often the system model is not known precisely and stochastic techniques are not effective. The scheduling problem, which consists of estimating the state of an uncertain process based on measurements obtained by switching a given set of noisy sensors, is addressed in [12]. This approach does not rely on stochastic models, but handles uncertainties that are modeled by unknown functions that satisfy integral quadratic constraints.

Nonlinearities within a system, such as model round off errors, colored noises, etc., can hinder the reconstruction of the state from measurements. Stochastic filters such as the Extended Kalman Filter (EKF) and Unscented Kalman Filter (UKF) address nonlinearities directly: the EKF linearizes the dynamics while the UKF propagates finite points through the nonlinear dynamics [5]. But both approaches ignore higher order terms of the nonlinearities. The designer can address these issues by typically "tunning" the process/sensor noise matrices in a somewhat ad hoc manner. By ignoring these higher order terms, the error covariance is not an accurate measurement of the bound on the state estimate, and thus makes them incompatible with current coordination approaches and robust control techniques that require bounded uncertainty information in their formulations in order to guarantee closed loop stability and performance [13].

This paper presents a procedure to compute hard bounds on state estimates of a nonlinear system. System nonlinearities are addressed by implementing a set of linear models each over a particular operating range, which are switched to minimize the uncertainty of the estimate. An Extended Set-Membership Filter (ESMF) is used to compute bounds for each of the system models [13]. In order to minimize computation and still achieve a desired level of uncertainty, the question of how many linear models should be implemented is also explored.

The paper is presented as follows. Section II describes how hard bounds on the state are obtained using the Extended Set-membership filter. Methods to create a hybrid state estimate trajectory and how to design for an uncertainty bound are presented in Section III. Finally an example is presented in Section IV to illustrate the proposed techniques.

II. The Extended Set-Membership Filter

The basis of set-membership estimation is to assume hard bounds on the noise, which allows hard bounds on the estimate of the state to be developed. In contrast, the Kalman Filter (or Extended Kalman Filter for nonlinear systems) assumes noise sources are stochastic and then recursively calculates the highest probability state estimate and covariance [3]. Set-membership estimation recursively computes an output set in which no point is more likely to be the actual state, but does guarantee that the actual state lies within this set. In the literature, set-membership methods have been derived using polytope and ellipsoidal methods. Ellipsoid methods require less information than polytope methods and

$$\hat{\mathbf{x}}_{\mathbf{k+1},\mathbf{k}} = f(\hat{\mathbf{x}}_{\mathbf{k},\mathbf{k}}) \quad (1)$$

$$\Sigma_{k+1,k} = A_k \frac{\Sigma_{k,k}}{1-\beta_k} A_k^T + \frac{\hat{Q}_{k,k}}{\beta_k} \quad (2)$$

$$\hat{\mathbf{x}}_{\mathbf{k+1},\mathbf{k+1}} = \hat{\mathbf{x}}_{\mathbf{k+1},\mathbf{k}} + \frac{\Sigma_{k+1,k}}{1-\rho_{k+1}} C_{k+1}^T \left[C_{k+1} \frac{\Sigma_{k+1,k}}{1-\rho_{k+1}} C_{k+1}^T + \frac{\hat{R}_{k+1}}{\rho_{k+1}} \right]^{-1} [\mathbf{y_{k+1}} - h(\hat{\mathbf{x}}_{\mathbf{k+1},\mathbf{k}})] \quad (3)$$

$$\bar{\Sigma}_{k+1,k+1} = \frac{\Sigma_{k+1,k}}{1-\rho_{k+1}} - \frac{\Sigma_{k+1,k}}{1-\rho_{k+1}} C_{k+1}^T \left[C_{k+1} \frac{\Sigma_{k+1,k}}{1-\rho_{k+1}} C_{k+1}^T + \frac{\hat{R}_{k+1}}{\rho_{k+1}} \right]^{-1} C_{k+1} \frac{\Sigma_{k+1,k}}{1-\rho_{k+1}} \quad (4)$$

$$\delta_{k+1} = [\mathbf{y_{k+1}} - h(\hat{\mathbf{x}}_{\mathbf{k+1},\mathbf{k}})]^T \left[C_{k+1} \frac{\Sigma_{k+1,k}}{1-\rho_{k+1}} C_{k+1}^T + \frac{\hat{R}_{k+1}}{\rho_{k+1}} \right]^{-1} [\mathbf{y_{k+1}} - h(\hat{\mathbf{x}}_{\mathbf{k+1},\mathbf{k}})] \quad (5)$$

$$\Sigma_{k+1,k+1} = (1-\delta_{k+1}) \bar{\Sigma}_{k+1,k+1} \quad (6)$$

$$A_k = \left. \frac{\partial f(\mathbf{x_k})}{\partial \mathbf{x}} \right|_{\mathbf{x_k}=\hat{\mathbf{x}}_{\mathbf{k},\mathbf{k}}}, C_{k+1} = \left. \frac{\partial h(\mathbf{x_k})}{\partial \mathbf{x}} \right|_{\mathbf{x_k}=\hat{\mathbf{x}}_{\mathbf{k},\mathbf{k}}} \quad (7)$$

are perhaps more intuitive because of their analogy to the covariance in stochastic estimation. The ellipsoidal method, as developed by Schweppe [14], is used in [13] to formulate the extended set-membership filter (ESMF) which extends set-membership estimation to dynamic nonlinear systems. The ESMF is chosen in this paper because it is well suited for on-line usage, does not make any assumptions on the type of noise (except that it is bounded), and calculates a non-conservative estimated set.

A. Basic Algorithm

Consider the discrete nonlinear state-space system:

$$\mathbf{x_{k+1}} = f(\mathbf{x_k}) + \mathbf{w_k} \quad (8)$$

$$\mathbf{y_{k+1}} = h(\mathbf{x_{k+1}}) + \mathbf{v_{k+1}} \quad (9)$$

where $\mathbf{x_k} \in \mathbb{R}^n$ is the state vector, $\mathbf{w_k} \in \mathbb{R}^n$ is the disturbance, $\mathbf{y_{k+1}} \in \mathbb{R}^{n_y}$ is the measurement, $\mathbf{v_{k+1}} \in \mathbb{R}^{n_y}$ is the sensor noise.

An ellipsoidal constraint of the form $[\mathbf{x}-\mathbf{y}]P^{-1}[\mathbf{x}-\mathbf{y}]^T \leq 1$ is represented by the notation $\mathbf{x} \in \Omega(\mathbf{y}, P)$. The initial state, $\mathbf{x_0}$, process noise, and sensor noise are assumed to be bounded by ellipsoids.

$$\mathbf{x_0} \in \Omega(\hat{\mathbf{x}}_\mathbf{0}, \Sigma_{0,0}) \quad (10)$$

$$\mathbf{w_k} \in \Omega(0, Q_k) \quad (11)$$

$$\mathbf{v_{k+1}} \in \Omega(0, R_{k+1}) \quad (12)$$

Linearizing Equation (8) about the current state estimate, $\hat{\mathbf{x}}_\mathbf{k}$, yields

$$\mathbf{x_{k+1}} = f(\hat{\mathbf{x}}_\mathbf{k}) + \left. \frac{\partial f(\mathbf{x_k})}{\partial \mathbf{x}} \right|_{\mathbf{x_k}=\hat{\mathbf{x}}_\mathbf{k}} (\mathbf{x_k} - \hat{\mathbf{x}}_\mathbf{k}) + O(\mathbf{x_k}^2) + \mathbf{w_k}. \quad (13)$$

The ESMF [13] combines the higher order terms and the process noise into one bound such that Equation (13) can be rewritten as

$$\mathbf{x_{k+1}} = f(\hat{\mathbf{x}}_\mathbf{k}) + \left. \frac{\partial f(\mathbf{x_k})}{\partial \mathbf{x}} \right|_{\mathbf{x_k}=\hat{\mathbf{x}}_\mathbf{k}} (\mathbf{x_k} - \hat{\mathbf{x}}_\mathbf{k}) + \hat{\mathbf{w}}_\mathbf{k} \quad (14)$$

where $\hat{\mathbf{w}}_\mathbf{k}$ is a new noise term that bounds both the original noise and the linearization remainder, $\hat{\mathbf{w}}_\mathbf{k} \in \Omega(0, \hat{Q}_k)$. A similar procedure applied on the measurement, Equation (9), yields $\hat{\mathbf{v}}_\mathbf{k+1} \in \Omega(0, V_{k+1})$. The procedure to combine the process and measurement noise with the linearization errors is based on interval mathematics and is discussed in Section II-B or described in detail in [13].

Given the initial conditions, Equation (10), the extended noise bounds calculated at each time step, $\hat{\mathbf{w}}_\mathbf{k}$ and $\hat{\mathbf{v}}_\mathbf{k+1}$, and the system dynamics, Equation (8), the state ellipsoid center, $\Omega(x_{k,k}, \Sigma_{k,k})$, can be estimated recursively by applying a linear set-membership filter [14].

The prediction step, Equations (1-2), is physically the addition of two ellipsoids, the augmented noise ellipsoid $\Omega(0, \hat{Q}_k)$ and the state uncertainty ellipsoid $\Omega(\hat{\mathbf{x}}_{\mathbf{k},\mathbf{k}}, , \Sigma_{k,k})$ rotated and scaled by A_k^T and A_k. The update step, Equations (3-6), is the intersection of two sets, the predicted state ellipsoid and the set described by the output equation $\Omega(\mathbf{y_{k+1}}, R_k)$. The actual state, $\mathbf{x_k}$, is then bounded by

$$[\mathbf{x_{k+1}} - \hat{\mathbf{x}}_\mathbf{k+1}]^T \Sigma_{k+1,k+1}^{-1} [\mathbf{x_{k+1}} - \hat{\mathbf{x}}_\mathbf{k+1}] \leq 1. \quad (15)$$

B. Defining Models and Bounding

Considering the scalar case for simplicity, rewriting Equation (13) yields

$$x_{k+1} = f(x_k)|_{x_k=\hat{x}_k} + \left. \frac{\partial f(x_k)}{\partial x} \right|_{x_k=\hat{x}_k} + \ldots + \left. \frac{f(x_k)^{n_r}}{n_r!} \right|_{x_k=\hat{x}_k} (x_k - \hat{x}_k)^{n_r} + R_{n_r}(x_k - \hat{x}_k, X_k) + w_k \quad (16)$$

where R_{n_r} is a remainder term, and f^{n_r} the n_rth derivative. Following Taylor's Theorem [13], the Lagrange remainder is written as

$$R_{n_r}(x_k, \hat{x}_k, X_k) = \frac{f^{(n_r+1)}(X_k)}{(n_r+1)!}(x_k - \hat{x}_k)^{n_r+1}. \quad (17)$$

The term X_k can take on any value over an interval for which $(x_k - \hat{x}_k)$ is defined. Therefore, Equation (17) can be bounded by an interval by simply defining the interval X_k and evaluation $R_{n_r}(x_k - \hat{x}_k, X_k)$ using interval mathematics.

For the proposed piecewise linear hybrid estimator, the nonlinear dynamics are linearized about the operating points. The models used in this formulation are defined by linearizing the nonlinear system dynamics, Equation (8), around N fixed operating points, $\overline{\mathbf{x}}^{\mathbf{i}}$. Evaluating Equation (7) at the operating points yields a set of system matrices, A_i, and output matrices, C_i.

Since linearization is done with respect to a set of fixed operating points the linearization error is a function of those points. Rewriting Equation (13) for the one-state case using a Lagrange remainder yields

$$x_{k+1} = f(x_k)|_{x_k=\overline{x}_i} + \left.\frac{\partial f(x_k)}{\partial x}\right|_{x_k=\overline{x}_i}(x_k - \overline{x}_i) \quad (18)$$

$$+\frac{1}{2}\frac{\partial^2 f(X_k)}{\partial x^2}(x_k - \overline{x}_i)^2 + w_k \quad (19)$$

where $\overline{x}_i$ denotes the i-th operating point. The linearization error, the fourth term on the right-hand side of Equation (19), is evaluated using interval mathematics which yields the interval $X^i_{R_k}$. In order to maintain guarantees on the bounds of the state estimates in a hybrid form of the ESMF, the transition of the bounds/uncertainties from one mode to the next must be addressed. In the hybrid case, the extrema of the current state ellipsoid, $\Omega(\overline{\mathbf{x}}^{\mathbf{i}}, \Sigma_{k,k})$, is centered at the operating point $\overline{\mathbf{x}}^{\mathbf{i}}$ and is defined as

$$\left[x_{(k,k),\pm}\right]^j = \left[\overline{x}^i_{k,k}\right]^j \pm \sqrt{\left[\Sigma_{k,k}\right]^{j,j}}, \quad (20)$$

where the superscript denotes the j-th state. The state interval bound becomes

$$[X_{k,k}]^j = \left[\left[x_{(k,k),-}\right]^j, \left[x_{(k,k),+}\right]^j\right]. \quad (21)$$

This interval is bounded using an ellipsoid that is not uniquely defined, but can be optimized by minimizing a metric of the ellipsoid. If the volume is minimized, the closed form solution is written as [13]

$$\left[\overline{Q}_{k,k}\right]^{j,j}_{R_k} = 2\left(\left[X_{R_k}\right]^j\right)^2 \quad (22)$$

if $j \neq m$, $\left[\overline{Q}^{j,j}_{k,k}\right] = 0$. The combined process noise bound, $\hat{Q}_{k,k}$, is found by adding the ellipsoids bounding the linearization error, Equation (22), and the process noise, Q_k.

$$\hat{Q}_{k,k} = \Omega_s(\overline{Q}_{k,k}, Q_k, \beta_Q) \quad (23)$$

where β_Q is a scalar, $0 < \beta_Q < 1$. The scalars β_k, ρ_{k+1} and β_Q are defined between 0 and 1 and can be optimized to find the smallest ellipsoid that bounds the addition ellipsoids. Having defined the combined process noise bound for N operating points, the ESMF equations can be applied recursively.

III. Model Switching

A hybrid or more specifically a switched dynamical system can be described by an ordinary differential equation of the form

$$\dot{\mathbf{x}}(t) = f_i(\mathbf{x}(t), \mathbf{u}(t)) \quad (24)$$

$$\mathbf{y}(t) = h_i(\mathbf{x}(t), \mathbf{u}(t)) \quad (25)$$

where $\mathbf{x}(t) \in \mathbb{R}^n$ is the state, for $i \in 1, 2, \ldots n$. $f_1(\cdot), \ldots, f_n(\cdot)$ and $h_1(\cdot), \ldots, h_n(\cdot)$ are continuous vector functions that describe the behavior and output of the system under different conditions. This model was created to more accurately describe systems in which a single vector function is not sufficient. Switching between the vector functions is typically done for control reasons such as to maintain stability or improve robustness. Linearizing f_i and h_i in Equations (24-25) about the i-th operating point results in the i-th model, Φ_i, composed of the matrices (A_i, B_i, C_i, D_i).

$$\Phi_i = \left[\begin{array}{c|c} A_i & B_i \\ \hline C_i & D_i \end{array}\right] \quad (26)$$

The discrete version of Equations (24,25) with process and measurement noise results in

$$\mathbf{x_{k+1}} = [A]_i\mathbf{x_k} + [B]_i\mathbf{u_k} + \mathbf{w_k} \quad (27)$$

$$\mathbf{y_{k+1}} = [C]_i\mathbf{x_k} + [D]_i\mathbf{u_k} + \mathbf{v_{k+1}} \quad (28)$$

where the subscript i denotes the i-th model.

A. Piecewise Linear Model Selection

It is proposed here to switch estimators based on the size of the uncertainty while also bounding the uncertainty through the mode transitions. The ESMF defines a bound in the form of a state ellipsoid, $\Omega\left(\overline{\mathbf{x}}^{\mathbf{i}}_{\mathbf{k}}, \Sigma_{k,k}\right)$, in which the true state lies (Equation (15)); the quality of the estimate can be assessed by evaluating the size of the bound. In the ESMF, the size of the bound is influenced by the measurement, the process and measurement noise, and the linearization error. In the hybrid formulation of the ESMF, the linearization error inherently increases as the system moves away from the operating points. The quality of the estimate is evaluated by defining a metric for the size of the uncertainty ellipsoid, $\Omega\left(\overline{\mathbf{x}}^{\mathbf{i}}_{\mathbf{k}}, \Sigma_{k,k}\right)$. Metrics that could be used to measure the size of the uncertainty include the trace, the determinant, and the maximum eigen value. In practice, the trace is often used for this purpose. The determinant of a matrix is proportional to the volume of the ellipsoid defined by the matrix. Used as a metric, the maximum eigen value indicates the largest size ellipsoid in one dimension.

TABLE I

MODEL SELECTION CRTIERIA.

	Metric
1	$tr(\Sigma_{k,k})$
2	$\lvert\Sigma_{k,k}\rvert$
3	max [eig($\Sigma_{k,k}$)]
4	$tr(\hat{Q}_k)$
5	$\lvert\hat{Q}_k\rvert$
6	max [eig($\hat{Q}_k$)]

An alternative set of metrics can be developed based on the bound on the linearization error, such as $\Omega\left(\overline{\mathbf{x}}^{\mathbf{i}}_{\mathbf{k}}, Q_{k,k}\right)$. This method isolates the influence of the linearization error on the size of the uncertainty. By not considering the measurement, $\mathbf{y_{k+1}}$, the metric immediately reacts to fluctuations in the linearization error. The metrics are applied to the state ellipsoid $\Omega\left(\overline{\mathbf{x}}^{\mathbf{i}}_{\mathbf{k}}, \Sigma_{k,k}\right)$ react more slowly as the information must first pass through the dynamics of the ESMF. All six metrics are summarized in Table I.

The hybrid estimator is then implemented by switching N ESMFs running based on each of the operating points. Depending on the measurement, noise, and linearization error, the quality of the estimate of each filter will vary. Switching is based on evaluating each filter using one of the metrics in Table I, which enables the hybrid estimator to minimize and bound uncertainty across the operating regions and transitions. The continuity assumptions of the ESMF are maintained because there are no discontinuities in the Hessian and Jacobian of all N filters.

B. Model Selection Based on Uncertainty

The size of the uncertainty in the hybrid estimator is a function of the number of operating points (N) as well as their location. Thus, the designer can choose either the number of filters (N) or size of uncertainty (Table I). The approach here is to use the Bersekas formulation of the set-membership filter [4] as opposed to the Schweppe formulation presented in Section II, because the state uncertainty matrix $\Sigma_{k,k}$ does not depend on the observation and will converge to a steady state value, i.e. $\lim_{k\to\infty} = \Sigma_{ss}$ [4]. It is noted that both approaches are outer bounding. The Bertsekas differs in how the state matrix is propagated, as shown in Equations (29-30).

$$\Sigma_{k,k} = \left[(1-\rho_{k+1})\,\overline{\Sigma}^{-1}_{k,k} + \rho_{k+1} C^T_{k+1} \hat{R}^{-1}_{k+1} C_{k+1}\right]^{-1} \tag{29}$$

$$\delta_k = (1-\beta_{k-1})\,(1-\rho_k)\,\delta_{k-1} + \left(z_k - C_k A_{k-1} \hat{x}_{k-1}\right)^T \tag{30}$$

with the initial condition, $\delta_0 = 0$. In the Bertsekas based ESMF, Equations (4,5) are replaced by Equations (29,30) respectively. The actual state $\mathbf{x_k}$ is bounded by $\Omega(\overline{\mathbf{x}}^{\mathbf{i}}, (1-\delta_{k+1})\Sigma^{-1}_{k+1,k+1})$.

A procedure is developed here to find the location of N linearization points used in the hybrid estimator based on the magnitude of the system's uncertainty. Defining the full range of operation to be $\widetilde{\mathbf{x}} = [\mathbf{x_{min}}, \mathbf{x_{max}}]$, the N the operating points inside the range are $\overline{\mathbf{x}}^{\mathbf{i}}$ for $i = \{1, ..., N\}$, the linearization error for j^{th} component of $f(\mathbf{x_k})$, Equation (19), and the i^{th} operating point from:

$$H^i_j(\mathbf{x_k}, \overline{\mathbf{x}}^{\mathbf{i}}) = (\mathbf{x_k} - \overline{\mathbf{x}}^{\mathbf{i}})^T \left.\frac{\partial^2 f_j(\mathbf{x_k})}{\partial \mathbf{x}^2}\right|_{\mathbf{x_k}=\overline{\mathbf{x}}^{\mathbf{i}}} (\mathbf{x_k} - \overline{\mathbf{x}}^{\mathbf{i}}). \tag{31}$$

The linearization error for the jth state equation of the hybrid estimator within the interval $\widetilde{\mathbf{x}}$ is found by minimizing the linearization over all N operating points:

$$\overline{H_j}(\mathbf{x_k}, \overline{\mathbf{x}}^{\mathbf{i}}, \ldots, \overline{\mathbf{x}}^{\mathbf{N}}) = \min_{\mathbf{x_k}\in\widetilde{\mathbf{x}}} \left(H^i_j(\mathbf{x_k}, \overline{\mathbf{x}}^{\mathbf{i}}), \ldots, H^N_j(\mathbf{x_k}, \overline{\mathbf{x}}^{\mathbf{N}})\right). \tag{32}$$

Placement of the operating points is then accomplished by minimizing a typical metric of the linearization error defined, Equation (32), by moving the location of the operating points.

Minimizing the area under $\overline{H}_j$ is inefficient because ultimately the maximum size of the uncertainty is a function of the largest value that H_i attains in $\widetilde{\mathbf{x}}$ and computations are wasted by calculating other points.

To directly minimize the maximum values of $\overline{H}_j$, the objective function is chosen so that placing the operating points is formulated as a nonlinear minimax optimization problem.

$$Q_{max} = \min_{\mathbf{x^i}\in\widetilde{\mathbf{x}}} \left(\max_{\mathbf{x}\in\widetilde{\mathbf{x}}} \left[\overline{H}_1, \ldots, \overline{H}_N\right]\right) \tag{33}$$

An added advantage of formulating the objective function as shown in Equation (33) is that H^i_j can be evaluated at $\mathbf{x_{min}}, \mathbf{x_{max}}, \mathbf{c_i}$, and the local minima of H^i_j that are found via differentiation or at the switching boundaries. The optimal value of the objective function, Equation (33), Q_{max}, is then the largest linearization error in the interval. Q_{max} is then used to find the steady state value of the state matrix Σ^{ss}. If this value is not within the desired range, then another operating point is added and the process is repeated.

The procedure to find the location and the minimum number of operating points to satisfy an uncertainty of Σ_{max} can be summarized as follows:

1) Solve Equations (2,4,29,30) with $\overline{Q}_{k,k} = 0$, to find the smallest steady state uncertainty, Σ^{ss}_{min} based on the chosen metric. This is the best steady state uncertainty since it is only due to noises in the system. If Σ_{max} is *greater* than Σ^{ss}_{min} then go on to step 2, else redefine Σ_{max}.
2) Add one operating point within $[\mathbf{x_{min}}, \mathbf{x_{max}}]$.
3) Solve the nonlinear minimax optimization problem, Equation (33).
4) Substitute Q_{max} and find the steady state uncertainty, Σ^{ss} using Equations (2,4, 29,30).
5) If $\Sigma^{ss} > \Sigma^{max}$ then go to step 2, else the location and number of operating points that meet the desired uncertainty has been found.

IV. Example

The procedure proposed in this paper is evaluated by implementing it on a model of the relative motion of two aircraft.

$$x_{r,k+1} = x_{r,k} + T[-v_{0,k} + v_{1,k}\cos\psi_{r,k} + \omega_0 y_{r,k}] \quad (34)$$

$$y_{r,k+1} = y_{r,k} + T[v_{1,k}\sin\psi_{r,k} - \omega_0 x_{r,k}] \quad (35)$$

$$\psi_{r,k+1} = \psi_{r,k} + T[\omega_1 - \omega_0] \quad (36)$$

Equations (34-36) depict the relative motion of aircraft 1 with respect to aircraft 0 (which is equivalent to fixing the origin of the relative motion of aircraft 1 and studying the motion of aircraft 1 with respect to aircraft 0). $(x_r, y_r, \psi_r) \subset \mathbb{R}^2 \times [-\pi, \pi]$ is the relative position and orientation of aircraft 1 with respect to aircraft 0 and v_i and ω_i are the linear and angular velocities of each aircraft. The control input is the linear velocity of aircraft 0, $u = v_0$, the disturbance is the linear velocity of aircraft 1, $d = v_1$, and T is the sampling time. This system is the discrete version of the model found in [8]. The sensor output is:

$$\mathbf{y_{k+1}} = \begin{bmatrix} y_{1,k+1} \\ y_{2,k+1} \end{bmatrix} = \begin{bmatrix} x_{r,k+1} \\ y_{r,k+1} \end{bmatrix} + \mathbf{v_{k+1}} \quad (37)$$

For this example, $v_1 = 10\ m/s$, $\omega_1 = 0.5\ rad/sec$, $v_0 = 0\ m/s$, and $\omega_0 = 0\ m/s$. The initial conditions for the systems are $\mathbf{x_0} = [0,0,0]$, while the sampling time for the system is 0.01 seconds. The noise for the system has the following form:

$$\eta = g(\overline{\eta}) \quad (38)$$

where $\eta \sim \mathcal{N}(0, \sigma^2)$ and $g(\cdot)$ is a transformation function that passes only values within $\pm\sigma$ of the mean. The result is a mixed random variable, η, that does not violate the assumptions of the ESMF since $\eta_k \in \Omega(0, \sigma^2)$. The variance for the process and measurement noise are $\text{diag}(0.01^2, 0.01^2, 0.01^2)$ and $\text{diag}(0.09^2, 0.09^2)$ respectively.

The trajectory for the system is shown in Figure 1. With a nonzero ω_1, the orientation of aircraft one starts at $[0,0,0]$ and rotates and moves to $\left[20, 20, \frac{\pi}{2}\right]$.

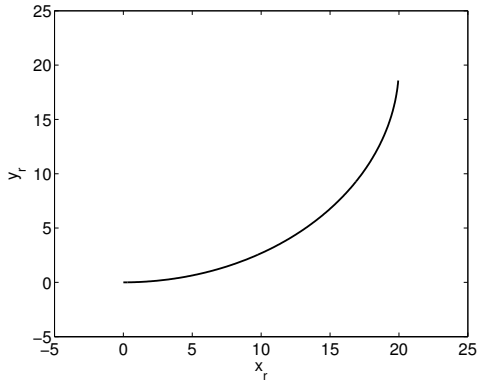

Fig. 1. Relative motion of plane 1 with initial conditions $[0\ 0\ 0]^T$.

The procedure described in Section III-B is used to find location of the operating points. Assume a design specification that requires the linearization uncertainty in $\psi(k)_r$ be smaller than 2.5 radians in the operating range, i.e. $\sqrt{\Sigma_{max}(3,3)} \leq 2.50$. From Step 1 in the process the steady state uncertainty is $\sqrt{\Sigma^{ss}_{min}(3,3)} = 1.86$ rad; therefore, the specification is feasible.

Defining now N operating points over the full system range:

$$\begin{bmatrix} 0 \\ 0 \\ \overline{\psi}_r^1 \end{bmatrix}, \begin{bmatrix} 0 \\ 0 \\ \overline{\psi}_r^2 \end{bmatrix}, \ldots, \begin{bmatrix} 0 \\ 0 \\ \overline{\psi}_r^N \end{bmatrix} \quad (39)$$

Computing the Hessians for this system reveals that uncertainty exists in two dimensions. The hybrid uncertainty for all three states is defined as

$$\overline{H}_1 = \min_{\mathbf{x_k} \in \widetilde{\mathbf{x}}} \left[(\psi_r - \overline{\psi}_r^1)^2 (T v_1 \cos\psi_r), \ldots, (\psi_r - \overline{\psi}_r^N)^2 (T v_1 \cos\psi_r) \right] \quad (40)$$

$$\overline{H}_2 = \min_{\mathbf{x_k} \in \widetilde{\mathbf{x}}} \left[(\psi_r - \overline{\psi}_r^1)^2 (T v_1 \sin\psi_r), \ldots, (\psi_r - \overline{\psi}_r^N)^2 (T v_1 \sin\psi_r) \right] \quad (41)$$

$$\overline{H}_3 = 0. \quad (42)$$

Equations (40-42) describe the linearization error in three dimensions for the system for N operating points. From Step 2, one operating point is added within $\widetilde{\mathbf{x}}$. Step 3 requires a solution to the nonlinear minimax optimization problem, Equation (33), which is in general nonconvex due to the structure of the objective function. Sequential quadratic programming [9] is used to minimize Equation (33) in MATLAB. The algorithm is initialized by selecting M points from a uniform distribution spanning $\widetilde{\mathbf{x}}$.

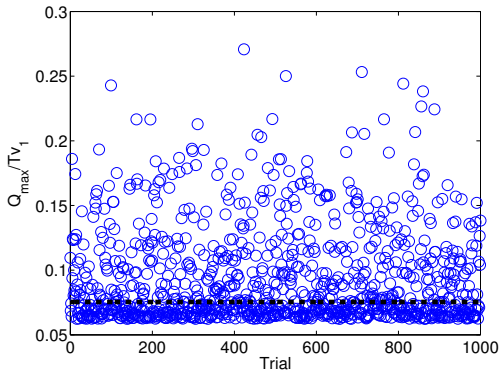

Fig. 2. Value of the objective at the solutions for 1000 trials of optimizing Equation (33) with three operating points. Points below the dashed line are below 110% of Q_{max}/Tv_1.

For comparison purposes, an exhaustive search over $\mathbf{x} \in \widetilde{\mathbf{x}}$ was conducted and the "best" value of $(\min_{\mathbf{x} \in \widetilde{\mathbf{x}}} Q_{max})$ is found

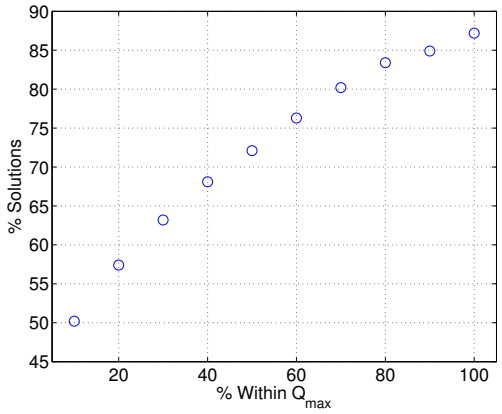

Fig. 3. Percentage of solutions within a percentage of Q_{max}.

to be 0.006. Although the optimization algorithm cannot guarantee convergence to a global minimum [9], Figure 2 shows the solutions found by initializing the problem with 1000 different points. The points below the dashed line in the figure are the points that are within 10% of the Q_{max} found from the exhaustive search. Figure 3 presents the percentage of optimized solutions that converge to a given percentage threshold of 0.006. The extreme nonlinear nature of the optimization makes it very difficult to find optimal solutions and as shown in Figure 2, the algorithm indeed does find nonoptimal solutions. However, Figure 3 suggests that, for a desired solution to be within 10% of $Q_{max} = 0.006$ the algorithm can be solved p times and $\frac{p}{2}$ of the solutions will be within the bound. It should be noted that Figures 2 and 3 display results for optimization over two dimensions and three operating points.

The best solution for Equation (33) using $N = 2$ results in a value of $Q^*_{max} = 0.129$ and $\sqrt{\Sigma^{ss}(3,3)} = 3.23$ for operating points $\bar{x}^1 = [0,0,0.39]$ and $\bar{x}^2 = [0,0,1.1]$. Because the uncertainty in the third state does not satisfy our requirements, Step 5 of the procedure states that another operating must be added and the optimization repeated. The solution with $N = 3$ results in $Q^*_{max} = 0.007$, $\sqrt{\Sigma^{ss}(3,3)} = 2.17$ for operating points at $\bar{\mathbf{x}}^{\mathbf{1}} = [0,0,0.22]$, $\bar{\mathbf{x}}^{\mathbf{2}} = [0,0,0.82]$, and $\bar{\mathbf{x}}^{\mathbf{3}} = [0,0,1.35]$. Because the uncertainty specification on ψ_r is met, there is no need to add more operating points.

The three operating found above are used to demonstrate the effect of uncertainty on the system. The resulting system matrices, A_i, for the system are shown below.

$$A_1 = \begin{bmatrix} 1 & 0 & -0.02 \\ 0 & 1 & 0.09 \\ 0 & 0 & 1 \end{bmatrix}, \quad A_2 = \begin{bmatrix} 1 & 0 & -0.07 \\ 0 & 1 & 0.07 \\ 0 & 0 & 1 \end{bmatrix},$$

$$A_3 = \begin{bmatrix} 1 & 0 & -0.10 \\ 0 & 1 & 0.02 \\ 0 & 0 & 1 \end{bmatrix}$$

Matrices, B_i, C_i, and D_i are the same for all three models and are shown in Equation (43),

$$B_i = \begin{bmatrix} \text{-T} \\ 0 \\ 0 \end{bmatrix}, C_i = \begin{bmatrix} 1 & 0 & 0 \\ 0 & 1 & 0 \end{bmatrix}, D_i = \begin{bmatrix} 0 \\ 0 \end{bmatrix} \tag{43}$$

for $i = \{1,2,3\}$.

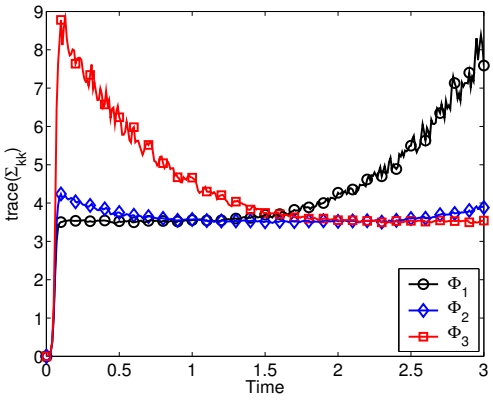

Fig. 4. Trace of the uncertainty for systems with constant plant models around 0, 45, and 90 degrees.

Figure 4 show the trace of the state ellipsoid as a function of time. The figures shows that close to the system's initial condition the filter implemented with the first operating point, $\bar{\mathbf{x}}^{\mathbf{1}} = [0,0,0.22]$, has a smaller trace than the other two models. As the system moves towards $\frac{\pi}{4}$ radians, the trace of the filter using the model defined around the second operating point, $\bar{\mathbf{x}}_{\mathbf{2}} = [0,0,0.82]$, decreases as the linearization error for this filter becomes smaller. The same can be said as ψ_r approaches $\frac{\pi}{2}$ for the filter using the third model around the operating point, $\bar{\mathbf{x}}_{\mathbf{3}} = [0,0,1.35]$.

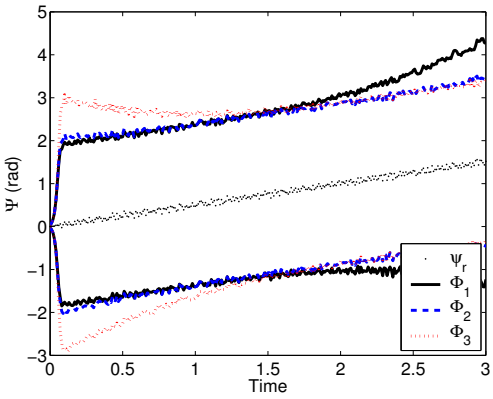

Fig. 5. Bounds on the orientation for constant plant models around 0.22, 0.82, and 1.35 radians.

The uncertainty on the third state for the three filters is shown in Figure 5. The magnitude of the uncertainty for each

of the filters changes as the linearization error evolves with respect to each operating point. Similar to the relationship shown in Figure 4, the uncertainty is smaller near each of the operating points.

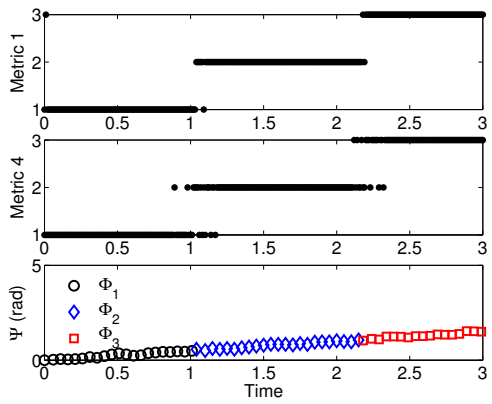

Fig. 6. Model chosen by considering the trace of the uncertainty and the trace of combined process noise ellipsoid.

Two of the switching criteria presented in Section III-A and Table I are compared in Figure 6. As ψ_r changes from 0 to $\frac{\pi}{2}$ each of the metrics selects which operating point is more appropriate. As seen in Figure 6 the switching is more consistent using $tr(\Sigma_{k,k})$, but relatively similar.

V. Conclusion

A method to define hard bounds on the state estimate using a set of switched linear models was presented. First, the bounding of the linearization error was adapted for use with set-membership with model switching. Then the Extended Set-Membership Filter was implemented to bound the state estimate for each model. Criteria that dictates when model switching occurs was defined in order to minimize uncertainty. The problem of determining the minimum number of operating points needed to guarantee a desired level of uncertainty was also discussed.

VI. Acknowledgements

This work was supported by the DARPA Software Enabled Control program, with Dr. Helen Gill and Dr. John Bay as DARPA Program Monitors and Mr. Raymond Bortner and Mr. James McDowell from AFRL as Contract Monitors. The DARPA IXO Grant (#F33615-99-C-3612) is administered through AFRL at Wright Patterson AFB.

VII. References

[1] R. Alur and D. Dill. A theory of timed automata. *Theoretical Computer Science*, 126(2):183–235, April 1994.

[2] A. Balluchi, L. Benvenuti, and M. Di Benedetto. Hybrid systems and the design of embedded controllers for automotive engine management. In *Proceedings of the 37th IEEE Conference on Decision and Control*, Tampa, FL, 1998.

[3] Y. Bar-Shalom, X. Rong Li, and T. Kirubarajan. *Estimation with Applications to Tracking and Navigation*. John Wiley and Sons, Inc., 2001.

[4] D. Bertsekas. *Dynamic Programming and Optimal Control*. Athena Scientific, 2000.

[5] M. Campbell and S. Brunke. Nonlinear estimation of aircraft models for on-line controls customization. In *IEEE Proceedings of Aerospace Conference*, Big Sky, MT, 2001.

[6] F. Ferrari-Trecate, D. Mignone, and M. Morari. Moving horizon estimation for hybrid systems. *IEEE Transactions on Automatic Control*, 47(10):1663–1676, October 2002.

[7] J. Lygeros, D. Godbole, and S. Sastry. Verified hybrid controllers for automated vehicles. *IEEE Transactions on Automatic Control*, 43(4):522–539, April 1998.

[8] J. Lygeros, C. Tomlin, and S. Sastry. On controller synthesis for nonlinear hybrid systems. In *Proceedings of the 37th IEEE Conference on Decision and Control*, Tampa, FL, December, 1998.

[9] J. Nocedal and S. Wright. *Numerical Optimization*. Springer-Verlag, New York, Inc., 1999.

[10] C. Rago, P. Willett, and Y. Bar-Shalom. Censoring sensor: a low communication rate scheme for distributed detection. *IEEE Transactions on Aerospace and Electronic Systems*, 32(2):554–568, April 1996.

[11] A. Savkin and R. Evans. *Hybrid Dynamical Systems*. Birkhauser, 2002.

[12] A. Savkin, R. Evans, and E. Skafidas. The problem of robust sensor scheduling. In *Proceedings of the 39th Conference on Decision and Control*, Sydney, Australia, 2000.

[13] E. Scholte and M. Campbell. A nonlinear set-membership filter for on-line applications. *Int. J. Robust Nonlinear Control*, 13(15):1337–1358, October 2003.

[14] F. Schweppe. *Uncertain Dynamic Systems*. Prentice Hall, 1973.

[15] E.D. Sontag. Nonlinear regulation: The piecewise linear approach. *IEEE Transactions on Automatic Control*, April, 1981.

[16] D. Sworder and J. Boyd. *Estimation Problems in Hybrid Systems*. Cambridge Univ. Press, 1999.

[17] C. Tomlin, G. Pappas, and S. Sastry. Conflict resolution for air traffic management: A study in multiagent hybrid systems. *IEEE Transactions on Automatic Control*, 43(4):509–521, April 1998.